Notes

Acetylene Polycyclotrimerization: Synthesis and Characterization of Ferrocene-Containing Hyperbranched Polyarylenes

Jianbing Shi,[†] Bin Tong,[†] Wei Zhao,[†] Jinbo Shen,[†] Junge Zhi,[‡] Yuping Dong,*[,†] Matthias Häussler,[§] Jacky W. Y. Lam,[§] and Ben Zhong Tang*[,§]

College of Materials Science & Engineering, College of Science, Beijing Institute of Technology, Beijing 100081, China, and Department of Chemistry, The Hong Kong University of Science & Technology, Clear Water Bay, Kowloon, Hong Kong, China

Received December 18, 2006
Revised Manuscript Received May 27, 2007

Introduction

Ferrocene possesses unique thermal and electrochemical properties and has been utilized as a versatile building block in the construction of advanced functional materials.[1] Ferrocene-containing conjugated polymers are of particular interest because of the potential of combining the unique redox properties of ferrocene with the novel electronic and optical properties of conjugated polymers.[2] Previous attempts to synthesize ferrocene-containing conjugated polymers have, however, often ended up obtaining insoluble, oligomeric products. The intractable oligomers can find little, if any, technological applications. It is thus of importance to develop new synthetic routes to ferrocene-containing conjugated polymers with macroscopic processability.

Hyperbranched polymers have attracted much attention because their unique molecular architectures have been found to impart new properties: for example, the polymers exhibit such rheological properties as high solubility and low viscosity.[3] Synthetic methodologies for hyperbranched polymers, however, have been rather limited. Common approaches include polycondensation of AB_n ($n \geq 2$) monomers[4] and self-condensing vinyl polymerization.[5] Because of the difficulty in the preparations of a monomer with two or more mutually reactive groups, other synthetic protocols such as $A_2 + B_3$ copolymerizations have been developed.[3] The stoichiometric requirements in such copolymerization systems are, however, practically difficult to meet.

Acetylene cyclotrimerization is an atom-economic reaction that transforms triple bonds to benzene rings.[6] We have worked on the synthesis of hyperbranched polyarylenes (*hb*-PAs) by the homo- and copolycyclotrimerizations of diynes and monoynes initiated by tantalum-, niobium-, and cobalt-based catalysts, with the aim of exploring new synthetic routes to conjugated hyperbranched polymers.[7,8] We have recently studied the copolycyclotrimerizations of 1,8-nonadiyne with (*E*)-2-(1-ferrocenyl)vinyl-*p*- or -*m*-phenylacetylene catalyzed by $TaBr_5$−Ph_4Sn, an example of which is shown in Scheme 1.[9] The electrochemical behaviors of the ferrocenyl units in the resultant *hb*-PAs are found to be similar to that of ferrocene because the insulating alkyl chains have effectively shut off the electronic communications between the phenyl rings in the polymer system. The polymers are nonluminescent, again due to their nonconjugated molecular structure. The polymers catastrophically decompose when heated to ∼500 °C because of the complete breakdown of the thermally liable alkyl linkers at the high temperatures.

Scheme 1

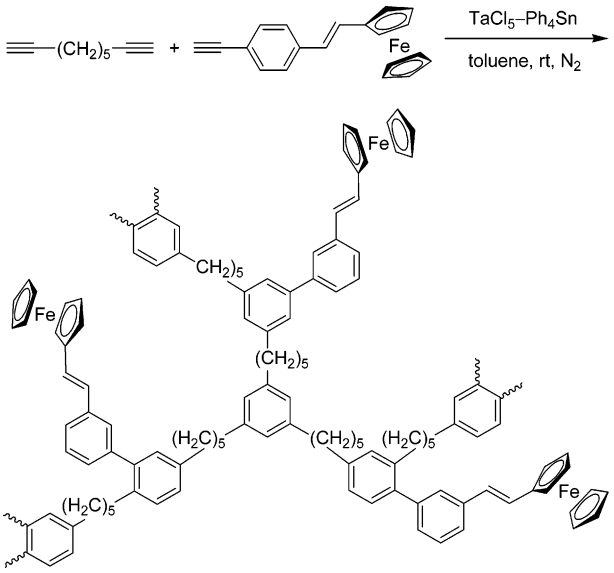

In this work, we designed and prepared a conjugated diyne monomer (A) by linking two acetylenic triple bonds together by a biphenyl bridge and investigated its copolycyclotrimerizations with (*E*)-2-(1-ferrocenyl)vinyl-*p*-phenylacetylene (B), in an effort to synthesize ferrocene-containing hyperbranched conjugated polymers (Scheme 2). The copolycyclotrimerization reactions were effected in toluene by $CpCo(CO)_2$−*hν*, giving soluble *hb*-PAs in good yields. Different from their nonconjugated counterparts (cf. Scheme 1), the *hb*-PAs are light-emitting, redox-active, and efficiently carbonized because of their core structures comprised of conjugated phenyl rings.

Experimental Section

The detailed synthetic procedures and characterization data for the monomers and polymers are given in the Supporting Information (SI).

Results and Discussion

Diyne A was prepared according to the synthetic route shown in Scheme 3. Palladium-catalyzed cross-coupling of diiodobi-

* To whom correspondence should be addressed: phone +86-10-6894-8982, Fax +86-10-6894-8982, e-mail chdongyp@bit.edu.cn (Y.P.D); phone +852-2358-7375, Fax +852-2358-1594, e-mail tangbenz@ust.hk (B.Z.T.).
[†] College of Materials Science & Engineering, Beijing Institute of Technology.
[‡] College of Science, Beijing Institute of Technology.
[§] The Hong Kong University of Science & Technology.

10.1021/ma062899w CCC: $37.00 © 2007 American Chemical Society
Published on Web 06/28/2007

Scheme 2

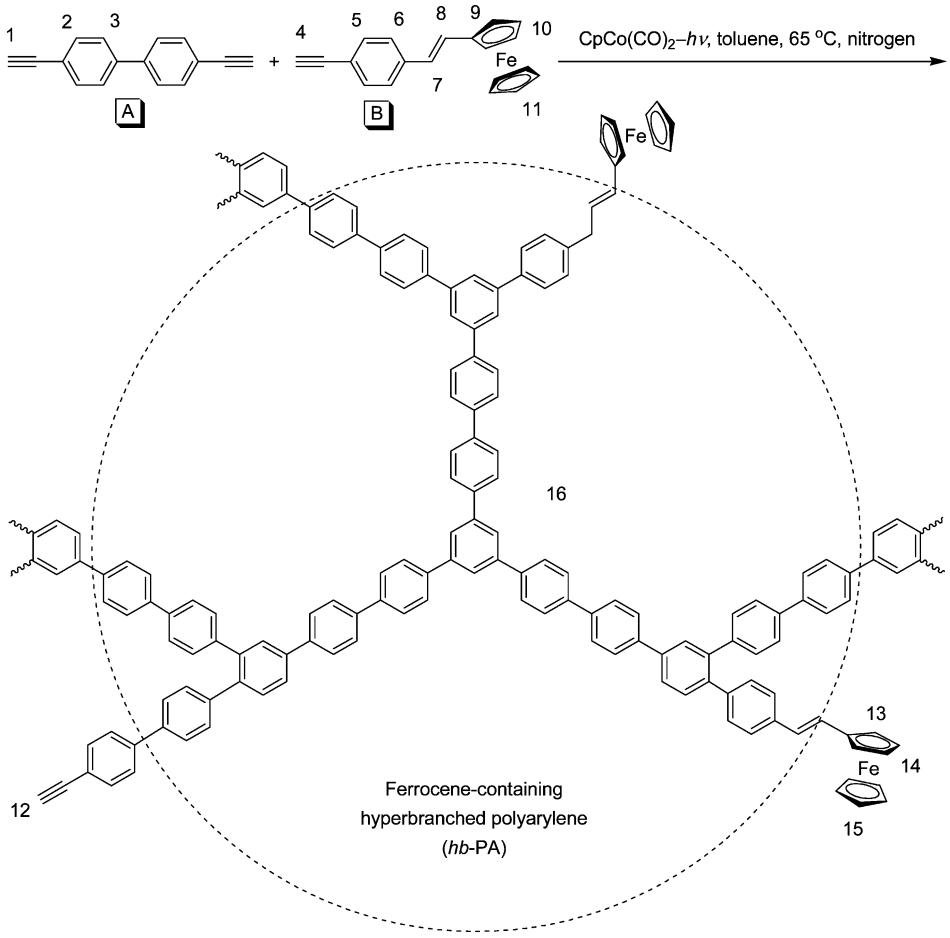

Scheme 3

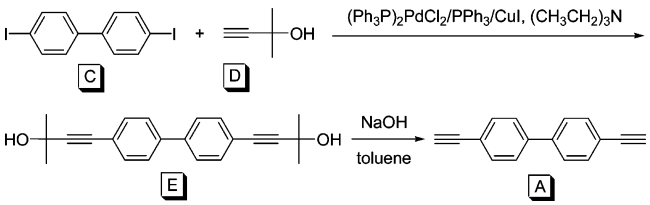

Scheme 4

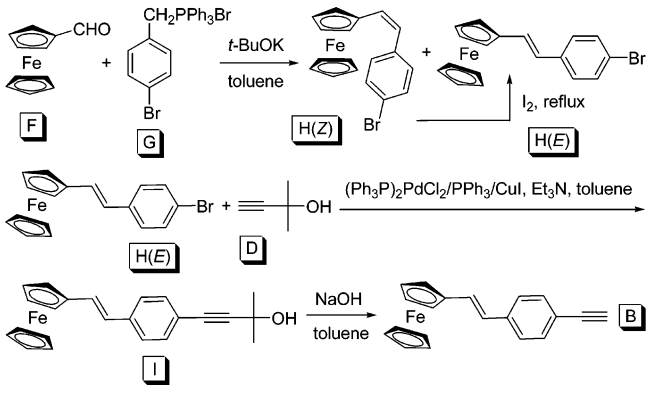

phenyl (C) with 2-methyl-3-butyn-2-ol (D), a terminal acetylene protected by a hydroxyisopropyl group, gave compound E, whose base-catalyzed deprotection afforded the desired terminal diyne monomer (A) in a high yield (~94%).

While monoyne B was prepared in our previous work,[9] we used a new scheme for its synthesis in this study (Scheme 4). Wittig reaction of ferrocenylaldehyde (F) with triphenylphosphonium ylide (G) gave an alkene (H) with *Z* and *E* conformations. The former conformer was converted to the latter by the iodine-catalyzed isomerization. By the similar coupling and deprotection reactions used in the synthesis of diyne A, the H(*E*) conformer was efficiently transformed to monoyne B.

After obtaining the diyne and monoyne monomers, we studied their polymerization behaviors. Since $CpCo(CO)_2$ can be handled with ease, we used its toluene solution to initiate copolycyclotrimerizations of the monomers. We first investigated how the catalyst concentration would affect the polymerization reaction. When a low catalyst concentration of 7.5 mM is used, copolycyclotrimerization of diyne A with monoyne B in a molar ratio [A]/[B] = 1:1 gives an *hb*-PA with a weight-average molecular weight (M_w) of 3000 in a moderate yield of ~54% (Table 1, no. 1). Raising the catalyst concentration to 15 mM makes the polymerization more effective, and a polymer with a higher M_w (4500) is obtained in a higher yield (70.0%). Further increasing the catalyst concentration to 30 mM results in deceases in the yield (68%) and M_w (3400), suggesting an optimal catalyst concentration of 15 mM. Delightfully, all the polymers are soluble in common organic solvents such as dichloromethane (DCM), chloroform, tetrahydrofuran (THF), and toluene.

We then followed the time course of the polymerization reaction. When the reaction time is increased from 0.5 to 6 h, the yield of the polymer is increased from 14.1% to 70% (cf. Table 1, nos. 4 and 2). A prolonged reaction (24 h) does not improve the polymer yield but results in the formation of partially soluble product. This is easy to understand: the probability for the unterminated acetylene groups in different

Table 1. Copolycyclotrimerization of Diyne A with Monoyne B[a]

no.	*hb*-PA	[A]:[B][b]	[cat.] (mM)	time (h)	yield (%)	M_w[c]	PDI[c]	*S*[d]
			Effect of Catalyst Concentration					
1	P**1**	1.0:1.0	7.5	6.0	53.8	3000	1.9	○
2	P**2**	1.0:1.0	15	6.0	70.0	4600	1.8	○
3	P**3**	1.0:1.0	30	6.0	62.8	3400	2.3	○
			Effect of Polymerization Time					
4	P**4**	1.0:1.0	15	0.5	14.1	2400	1.6	○
5	P**5**	1.0:1.0	15	2.0	38.0	3200	2.0	○
6	P**6**	1.0:1.0	15	24.0	67.1	4200	2.3	△
			Effect of Comonomer Feed Ratio					
7	P**7**	0.5:1.0	15	6.0	45.6	5300	2.1	○
8	P**8**	3.0:1.0	15	6.0	54.6	5000	1.9	○
9	P**9**	6.0:1.0	15	6.0	64.0	4700	1.8	○
10	P**10**	10.0:1.0	15	6.0	72.5	5200	1.8	△

[a] Carried out in toluene at 65 °C under nitrogen using $CpCo(CO)_2-h\nu$ as catalyst. [b] Molar ratio of diyne A and monoyne B in the comonomer feed mixture; total [−C≡CH] = 0.15 M. [c] Estimated by GPC in THF on the basis of a polystyrene calibration. PDI = polydispersity index (M_w/M_n). [d] Solubility (*S*) tested in common organic solvents such as toluene, DCM, chloroform, and THF. Symbols: ○ = completely soluble and △ = partially soluble.

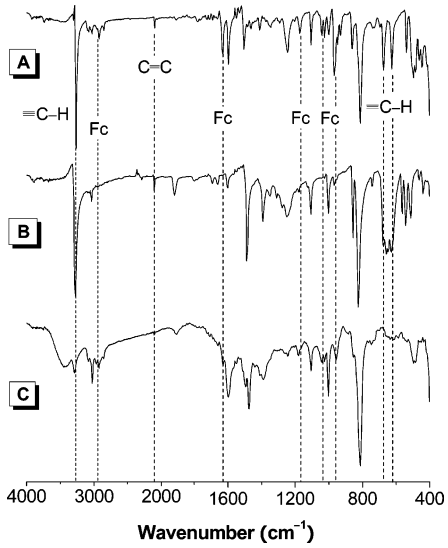

Figure 1. IR spectra of (A) diyne A, (B) monoyne B, and (C) polymer P**2** (sample from Table 1, no. 2).

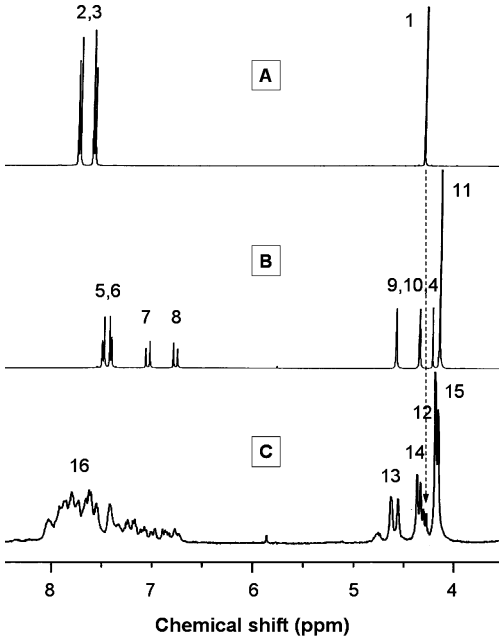

Figure 2. ^{1}H NMR spectra of (A) diyne A, (B) monoyne B, and (C) polymer P**2** (sample taken from Table 1, no. 2) in DMSO-d_6.

hb-PAs to react with each other (or to cross-link) should increase with an increase in the reaction time.

We finally studied the effect of molar ratio of the comonomer mixture on the polycyclotrimerization reaction. The molecular weights of the *hb*-PAs are almost independent of the molar feed ratios (Table 1, nos. 2 and 7−10). On the other hand, the polymer yield is generally increased with an increase in the molar ratio: when the A/B ratio is increased from 0.5:1 to 10:1, the polymer yields is raised from 45.6% to 72.5%. In the reaction mixture, monoyne B does not only work as a terminator for the propagating species but also undergo self-cyclotrimerization. The resultant low molecular weight compounds are washed away during the purification processes of the polymer products by precipitation, which thus lower the polymer yields.

The molecular weights of all the polymers measured by GPC are relatively low. One possible reason for the low M_w values is that hyperbranched polymers, when calibrated by linear polystyrene standards, usually give underestimated molecular weights due to their three-dimensional molecular architecture.[10] The real molecular weights of the *hb*-PAs could be much higher than the relative values estimated from the GPC analysis. All the polymers show the most probable molecular weight distributions, with their polydispersity indexes being in the range of 1.6−2.3.

The *hb*-PAs were analyzed spectroscopically, which gave satisfactory data well corresponding to their expected molecular structures. An example of the IR spectrum of P**2** is shown in Figure 1; those of their monomers are given in the same figure for comparison. The monomers show ≡C−H, C≡C, and ≡C−H bands at 3273−3264, 2105−2099, and 630−625 cm^{-1}, respectively (Figure 1, panels A and B), which become very weak in the spectrum of their copolymer (Figure 1C), indicating that most of the triple bonds have been consumed by the polycyclotrimerization reaction. The ferrocene-associated vibration bands at 2969, 1628, 1167, 1036, and 967 cm^{-1} are observed in the spectra of the polymer, proving that the copolycyclotrimerization reaction has proceeded as expected and has been harmless to the ferrocenyl group.

Figure 2 shows the ^{1}H NMR spectra of copolymer P**2** and monomers A and B. All the resonance peaks in the copolymer can be readily assigned. Compared with those of its monomers, the peaks of P**2** are broader due to its rigid molecular structure and irregular regioisomeric structure. The resonance peaks of the acetylenic protons of diyne A and monoyne B are located at δ 4.29 and 4.21, respectively. The acetylenic peaks are very weak in the spectrum of their copolymer, again proving that the triple bonds have been consumed by the copolycyclotrimerization reaction. The three resonance peaks of the protons of cyclopentadienyl (Cp) rings in the ferrocene units can be easily

Table 2. Electrochemical and Thermal Properties of Ferrocene-Containing Hyperbranched Polyarylenes

no.	*hb*-PA	f_B[a]	F_B[b]	i_{pa} (μA)	i_{pc} (μA)	E_{pa} (V)	E_{pc} (V)	$E_{1/2}$[c] (V)	T_d[d] (°C)	W_r[e] (%)
1	**P7**	0.67	0.54	10.23	−14.34	0.435	0.357	0.396	394	76.6
2	**P2**	0.50	0.44	9.05	−12.01	0.428	0.356	0.392	428	80.9
3	**P8**	0.25	0.21	7.37	−7.68	0.422	0.359	0.391	436	82.3
4	**P9**	0.14	0.11	6.95	−6.80	0.423	0.362	0.393	*f*	*f*
5	**P10**	0.09	*g*	6.41	−6.32	0.425	0.362	0.394	451	85.5

[a] Molar fraction of monoyne B in the comonomer feed mixture. [b] Molar fraction of monoyne unit in the *hb*-PA calculated from ^{1}H NMR spectral data using eq 1. [c] Formal redox potential; $E_{1/2} = (E_{pc} + E_{pa})/2$. [d] Degradation temperature (for 5% weight loss). [e] Weight residue (after pyrolysis at 1000 °C). [f] Not determined. [g] Not available because of the partial solubility of the polymer.

seen in the spectra of P**2** at δ 4.58, 4.35 and 4.16, well corresponding to those of monomer B. The intensities of these three peaks are decreased when the feed ratio of A is increased (Figure S1, Supporting Information).

To gain more insights into the polymer structure, the areas of the resonance peaks were integrated and analyzed. The resonance peaks of the protons of the unsubstituted Cp ring at δ ~4.16 (peak 15 in Figure 2C) is separated from those of the substituted Cp ring at δ ~4.35 (peak 14) and ~4.58 (peak 13). The resonance peaks of *hb*-PA in the chemical shift region of δ 6.77−8.07 (peak 16) are from several sources: the protons of the phenyl rings from the diyne and monoyne units, the protons of the vinyl group from the monoyne unit, and the protons of the phenyl rings formed in the polycyclotrimerization reaction. The molar fraction of the monoyne unit in the *hb*-PA (F_B) can thus be calculated from the NMR spectral data by the following equation:

$$\frac{5F_B}{7F_B + 10(1 - F_B)} = \frac{A_{15}}{A_{12} + A_{16}} \quad (1)$$

where A_{15}, A_{12}, and A_{16} are the integrated areas of the resonance peaks of the protons of the unsubstituted Cp ring at δ ~4.16, the unreacted terminal acetylene at δ ~4.29, and the phenyl and vinyl groups in the chemical shift region of δ 6.77−8.07. The calculated results of the *hb*-PAs are given in Table 2. The F_B value gradually gets close to that of the molar fraction of monoyne B in the comonomer feed mixture (f_B) with a decrease in f_B because the probability for the formation of small cyclotrimers from monoyne B is progressively decreased.

After characterizing the molecular structures of the *hb*-PAs, we investigated their optical and thermal properties. Polymer P**10**, prepared from a comonomer mixture with an [A]/[B] ratio of 10:1, shows an absorption peak (λ_{max}) at 312 nm (Figure 3A), which is 23 nm bathochromically shifted from that of diyne A (λ_{max} = 289 nm).[11] Clearly, the formation of new benzene ring by the cyclotrimerization of three triple bonds is the cause of this red shift because it generates an *hb*-PA with a π-conjugated structure. With an increase in F_B, the λ_{max} value gradually shifts to longer wavelengths, with P**7** showing a λ_{max} value as high as 328 nm. Interestingly, the increase in λ_{max} is directly proportional to the change in f_B (Figure 3A, inset), suggesting that the incorporation of the monoyne units, which carries a conjugated ferrocenylvinylphenyl group, helps enhance the extent of conjugation in the *hb*-PA system. All the *hb*-PAs exhibit a weak shoulder at around 470 nm, assignable to the d−d transition within the ligand field formalism of conjugated ferrocene, further confirming the successful incorporation of the ferrocene unit into the polymer structure.[12]

The UV absorption spectra of typical *hb*-PAs are compared with those of the simple blends of their comonomers with the same molar ratios in Figure 3B. The absorption spectrum of P**2** peaks at 323 nm, which is 29 nm red-shifted from the λ_{max} value of its corresponding comonomer mixture with an A/B ratio of

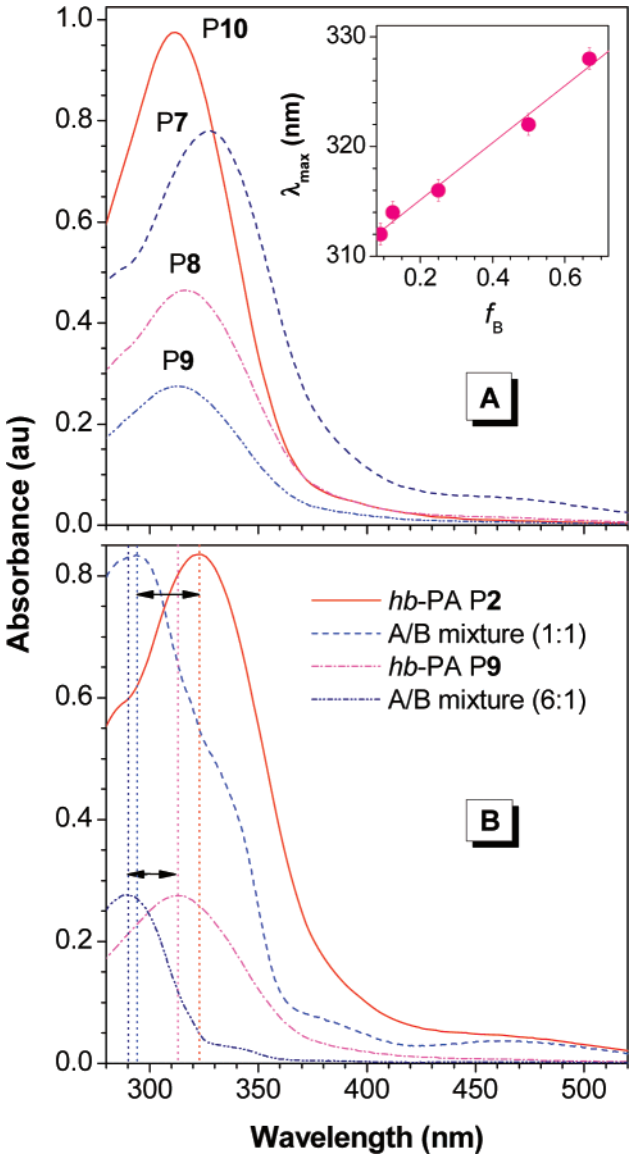

Figure 3. (A) Absorption spectra of DCM solutions (10 μg/mL) of hyperbranched polyarylenes. Inset: relationship between absorption maximum (λ_{max}) and molar fraction of monoyne B in the comonomer feed mixture (f_B). (B) Comparison between the absorption spectra of hyperbranched polyarylenes and those of their corresponding monomer mixtures.

1:1. Similarly, the absorption spectrum of P**9** (λ_{max} = 313 nm) is bathochromically shifted from that of its corresponding comonomer mixture (λ_{max} = 290 nm). These comparison data clearly indicate that the knitting of the diyne and monoyne units in the three-dimensional space through the formation of benzene rings has generated *hb*-PAs with a conjugated molecular structure.

The conjugated molecular structure of the *hb*-PAs enables them to emit light upon photoexcitation, in contrast to their

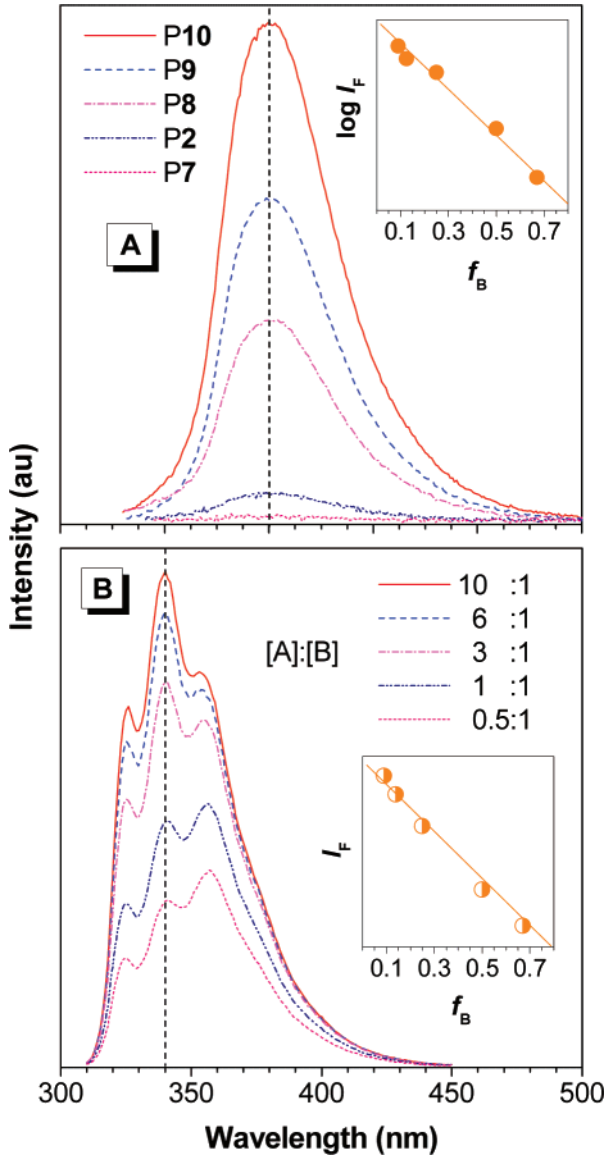

Figure 4. Emission spectra of DCM solutions (10 μg/mL) of (A) hyperbranched polyarylenes and (B) comonomer mixtures. Excitation wavelengths: (A) 320 and (B) 290 nm. Insets: relationships between fluorescence peak intensity (I_F) and molar fraction of monoyne B (f_B) for (A) hyperbranched polyarylenes and (B) comonomer mixtures.

nonconjugated counterparts synthesized in our previous work (cf. Scheme 1), which were all nonemissive.[9] The spectra of the *hb*-PAs show no fine structures, typical of polymer emissions (Figure 4A). The spectra are peaked at 400 nm (λ_{em}) and are intensified in the order of P**7** to P**10**. A semilog plot of fluorescence peak intensity (I_F) vs f_B gives a straight line, implying that the conjugated diyne units in the *hb*-PA are the emitting species and that the ferrocene-containing monoyne units are the quenching centers. Indeed, ferrocene is a well-known quenching species.[13]

Fluorescence spectra of DCM solutions of the comonomer mixtures are well structured, characteristic of small molecule emissions (Figure 4B). They are all blue-shifted from those of their corresponding polymers, with $\Delta\lambda_{em}$ up to 60 nm, proving that the *hb*-PAs are more conjugated than their monomers. An interesting observation is that the comonomer mixtures emit no recordable lights when excited at 320 nm, in contrast to the fact that this excitation can induce the polymers to emit. This again confirms that the polymers are more conjugated. The I_F-f_B plot for the comonomer mixtures gives a linear line, instead

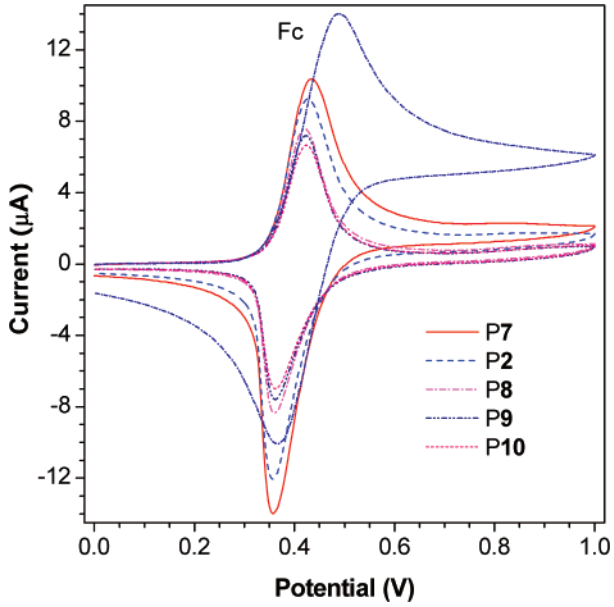

Figure 5. Cyclic voltammograms of hyperbranched polyarylenes measured at 25 °C in DCM solutions. Data for ferrocene (Fc) are shown for comparison.

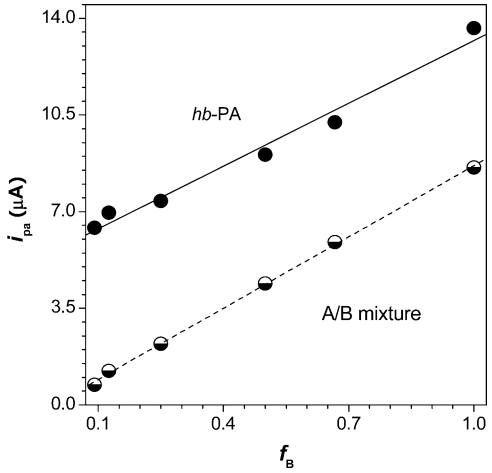

Figure 6. Plot of anodic current (i_{pa}) vs molar fraction of B (f_B) for the hyperbranched polyarylenes and the comonomer mixtures.

of a semilog one, indicating that the fluorescence is less efficiently quenched by the ferrocene units in the comonomer mixture. Diyne A and monoyne B are physically blended and chemically bonded in the comonomer mixtures and hyperbranched polymers, respectively. The intimate meld of the diyne units with the monoyne units in the hyperbranched polymers at the molecular level facilitates energy transfer, thus making the quenching by the ferrocene units a more efficient process.

Electrochemical properties of the *hb*-PAs were investigated by cyclic voltammetry. All the *hb*-PAs display chemically reversible ferrocene/ferricinium redox couples (Figure 5). Similar to their parent form of ferrocene, the polymers exhibit single oxidation waves in the range of 0−1 V (vs SCE). The half-wave potentials ($E_{1/2}$) of the *hb*-PAs are in a small window (0.391−0.396 V), being practically independent of the polymer compositions (Table 1). This suggests that the ferrocenyl units in the *hb*-PAs all possess the similar redox potentials due to the lack of direct interactions between the metal centers.[14] The $E_{1/2}$ values of the *hb*-PAs are, however, smaller than those (0.448−0.459 V) of their corresponding comonomer mixtures (Table S1, Supporting Information) and those (0.57−0.61 V) of their nonconjugated counterparts (cf. Scheme 1).[9] Clearly,

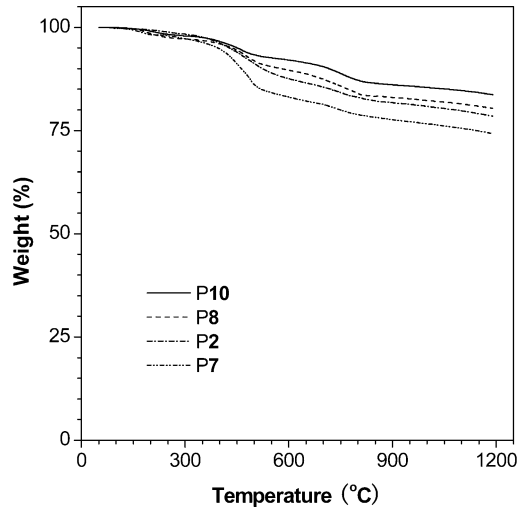

Figure 7. TGA thermograms of hyperbranched polyarylenes recorded under nitrogen at a heating rate of 10 °C/min.

the ferrocene units are oxidized more easily when incorporated into a conjugated polymer structure. The charges may have been stabilized by the delocalization effect in the conjugated system.

The oxidation wave is reversible, and the currents increase with an increase in the ferrocene content. Plotting the peak current (i_{pa}) against f_B gives a linear line (Figure 6). The slope of the $i_{pa}-f_B$ plot for the *hb*-PAs is similar to that for their corresponding comonomer mixtures, but the absolute currents in the former are higher than those in the latter. The electronic conjugation in the *hb*-PAs may have helped increase the diffusion coefficient, hence the observed constantly higher i_{pa} values in the polymer system.

Thermal stability of the *hb*-PAs was evaluated by thermogravimetric analysis (TGA). As can be seen from Figure 7, the polymers show excellent thermal stability, losing merely 5% of their weights when heated to temperatures in the vicinity of 400 °C (Table 1). The polymers are ceramized in high yields (up to ~86%) when pyrolyzed at 1000 °C for 1 h under nitrogen. The thermal stability increases with an increase in F_A due to the ready carbonization or graphitization of the phenyl rings. However, even the polymer with the highest ferrocene content (**P7**) still gives a char yield of ~77%, thanks to the "cage effect" of its hyperbranched molecular architecture.[15] After pyrolysis, the residues can be attracted to a bar magnet, probably due to the formation of iron nanoparticles inside the chars.[15] Detailed magnetic studies are underway and will be reported in a separate paper.

Conclusion

Ferrocene-containing conjugated *hb*-PAs have been synthesized by one-pot copolycyclotrimerizations of a biphenyldiyne with a ferrocenylmonoyne. The polymers are soluble. The conjugated structures of the *hb*-PAs are confirmed by comparing their optical and electrochemical properties with those of their comonomer mixtures and their nonconjugated counterparts.[9] The polymers are thermally stable and can be pyrolytically transformed into magnetic ceramics in high yields. The processable and stable *hb*-PAs with electronic conjugation and unique optical, redox, and thermal properties may find an array of high-tech applications as advanced functional materials.

Acknowledgment. This work was partially supported by the National Science Foundation of China (20474007 and 20634020).

Supporting Information Available: Synthesis procedures and characterization data for diyne A, monoyne B, and their polymers *hb*-PAs; electrochemical data for the comonomer mixtures. This material is available free of charge via the Internet at http://pubs.acs.org.

References and Notes

(1) (a) Plenio, H.; Hermann, J.; Leukel, J. *Eur. J. Inorg. Chem.* **1998**, 2063. (b) Kurihara, M.; Hirooka, A.; Kume, S. *J. Am. Chem. Soc.* **2002**, *124*, 8800. (c) Gibson, V. C.; Long, N. J.; Oxford, P. J. *Organometallics* **2006**, *25*, 1932.

(2) (a) Abd-El-Aziz, A. S. *Macromol. Rapid Commun.* **2002**, *23*, 995. (b) Nguyen, P.; Gomez-Elipe, P.; Manners, I. *Chem. Rev.* **1999**, *99*, 1515. (c) Abd-El-Aziz, A. S.; Manners, I. *J. Inorg. Organomet. Polym. Mater.* **2005**, *15*, 157. (d) Abd-El-Aziz, A. S.; Todd, E. K.; Okasha, R. M.; Shipman, P. O.; Wood, T. E. *Macromolecules* **2005**, *38*, 9411. (e) Foucher, D. A.; Tang, B. Z.; Manners, I. *J. Am. Chem. Soc.* **1992**, *114*, 6246. (f) Kloninger, C.; Rehahn, M. *Macromolecules* **2004**, *37*, 1720. (g) Temple, K.; Kulbaba, K.; Power-Billard, K. N.; Manners, I.; Leach, K. A.; Xu, T.; Russell, T. P.; Hawker, C. J. *Adv. Mater.* **2003**, *15*, 297. (h) Eitouni, H. B.; Balsara, N. P. *J. Am. Chem. Soc.* **2004**, *126*, 7446.

(3) Watson, M. D.; Fechtenkötter, A.; Müllen, K. *Chem. Rev.* **2001**, *101*, 3819.

(4) (a) Kim, Y. H.; Webster, O. W. *J. Am. Chem. Soc.* **1990**, *112*, 4592. (b) Kim, Y. H.; Webster, O. W. *Macromolecules* **1992**, *25*, 5561.

(5) Frèchet, J. M.; Henmi, M.; Gitsov, I.; Aoshima, S.; Leduc, M. R.; Grubbs, R. B. *Science* **1995**, *269*, 1080.

(6) *Modern Acetylene Chemistry*; Stang, P. J.; Diederich, F.; Eds.; VCH: Weinheim, 1995.

(7) (a) Zheng, R.; Dong, H.; Peng, H.; Lam, J. W. Y.; Tang, B. Z. *Macromolecules* **2004**, *37*, 5196. (b) Xu, K. T.; Peng, H.; Sun, Q. H.; Dong, Y. P.; Salhi, F.; Luo, J. D.; Chen, J. W.; Huang, Y.; Zhang, D. Z.; Xu, Z. D.; Tang, B. Z. *Macromolecules* **2002**, *35*, 5821. (c) Peng, H.; Cheng, L.; Luo, J.; Xu, K. T.; Sun, Q. H.; Dong, Y. P.; Salhi, F.; Lee, P. P.; Chen, J. W.; Tang, B. Z. *Macromolecules* **2002**, *35*, 5349.

(8) (a) Häussler, M.; Tang, B. Z. *Adv. Polym. Sci.* **2007**, *209*, in press (DOI 10.1007/12_2007_112). (b) Häussler, M.; Dong, H. C.; Lam, J. W. Y.; Zheng, R.; Qin, A.; Tang, B. Z. *Chin. J. Polym. Sci.* **2005**, *23*, 567. (c) Häuβler, M.; Lam, J. W. L.; Zheng, R.; Peng, H.; Luo, J. D.; Chen, J. W.; Law, C. C.; Tang, B. Z. *C. R. Chim.* **2003**, *6*, 833.

(9) Li, Z.; Lam, J. W. Y.; Dong, Y. Q.; Dong, Y. P.; Sung, H. H. Y.; Williams, I. D.; Tang, B. Z. *Macromolecules* **2006**, *39*, 6458.

(10) Harth, E. M.; Hecht, S.; Helms, B.; Malmstrom, E. E.; Frechet, J. M. J.; Hawker, C. J. *J. Am. Chem. Soc.* **2002**, *124*, 3926.

(11) Liu, L.; Poon, S.-Y.; Wong, W.-Y. *J. Organomet. Chem.* **2005**, *690*, 5036.

(12) Elsner, O.; Ruiz-Molina, D.; Rovira, C.; Veciana, J. *J. Organomet. Chem.* **2001**, *637*, 251.

(13) Cao, W.; Ferrance, J. P.; Demas, J.; Landers, J. P. *J. Am. Chem. Soc.* **2006**, *128*, 7573.

(14) (a) Jayakumar, N. K.; Bharathi, P.; Thayumanavan, S. *Org. Lett.* **2004**, *6*, 2547. (b) Stone, D. L.; Smith, D. K.; McGrail, P. T. *J. Am. Chem. Soc.* **2002**, *124*, 856. (c) Labande, A.; Ruiz, J.; Astruc, D. *J. Am. Chem. Soc.* **2002**, *124*, 1782. (d) Cardona, C. M.; McCarley, T. D.; Kaifer, A. E. *J. Org. Chem.* **2000**, *65*, 1857. (e) Chebny, V. J.; Dhar, D.; Lindeman, S. V.; Rathore, R. *Org. Lett.* **2006**, *8*, 5041. (f) Matas, J.; Uriel, S.; Peris, U.; Llusar, R.; Houbrechts, S.; Persoons, J. *J. Organomet. Chem.* **1998**, *562*, 197. (g) Imaoka, T.; Tanaka, R.; Arimoto, S.; Sakai, M.; Fujii, M.; Yamamoto, K. *J. Am. Chem. Soc.* **2005**, *127*, 13896.

(15) (a) Häussler, M.; Sun, Q.; Xu, K.; Lam, J. W. Y.; Dong, H.; Tang, B. Z. *J. Inorg. Organomet. Polym. Mater.* **2005**, *15*, 67. (b) Häussler, M.; Zheng, R.; Lam, J. W. Y.; Tong, H.; Dong, H.; Tang, B. Z. *J. Phys. Chem. B* **2004**, *108*, 10645. (c) Sun, Q.; Xu, K.; Peng, H.; Zheng, R.; Häussler, M.; Tang, B. Z. *Macromolecules* **2003**, *36*, 2309. (d) Sun, Q.; Lam, J. W. Y.; Xu, K.; Xu, H.; Cha, J. A. P.; Wong, P. C. L.; Wen, G.; Zhang, X.; Jing, X.; Wang, F.; Tang, B. Z. *Chem. Mater.* **2000**, *12*, 2617.

MA062899W